Author Manuscript

Author Manuscript

Author Manuscript

Author Manuscript

HHS Public Access

Author manuscript

Nat Med. Author manuscript; available in PMC 2020 March 09.

Published in final edited form as:

Nat Med. 2019 September ; 25(9): 1415–1421. doi:10.1038/s41591-019-0561-9.

Liquid versus tissue biopsy for detecting acquired resistance and tumor heterogeneity in gastrointestinal cancers

Aparna R. Parikh[*,1], **Ignaty Leshchiner**[*,2], **Liudmila Elagina**[*,2], **Lipika Goyal**[1], **Chaya Levovitz**[3], **Giulia Siravegna**[4,5], **Dimitri Livitz**[2], **Kahn Rhrissorrakrai**[3], **Elizabeth E. Martin**[2], **Emily E. Van Seventer**[1], **Megan Hanna**[2], **Kara Slowik**[2], **Filippo Utro**[3], **Christopher J. Pinto**[1], **Alicia Wong**[2], **Brian P. Danysh**[2], **Ferran Fece de la Cruz**[1], **Isobel J. Fetter**[1], **Brandon Nadres**[1], **Heather A. Shahzade**[1], **Jill N. Allen**[1], **Lawrence S. Blaszkowsky**[1], **Jeffrey W. Clark**[1], **Bruce Giantonio**[1], **Janet E. Murphy**[1], **Ryan D. Nipp**[1], **Eric Roeland**[1], **David P. Ryan**[1], **Colin D. Weekes**[1], **Eunice L. Kwak**[1], **Jason E. Faris**[1], **Jennifer Y. Wo**[1], **François Aguet**[2], **Ipsita Dey-Guha**[1], **Mehlika Hazar-Rethinam**[1], **Dora Dias-Santagata**[1], **David T. Ting**[1], **Andrew X. Zhu**[1], **Theodore S. Hong**[1], **Todd R. Golub**[2,6,7], **A. John Iafrate**[1], **Viktor A. Adalsteinsson**[2], **Alberto Bardelli**[4,5], **Laxmi Parida**[3], **Dejan Juric**[1], **Gad Getz**[#,1,2,8], **Ryan B. Corcoran**[#,1]

[1]Massachusetts General Hospital Cancer Center and Department of Medicine, Harvard Medical School, Boston, Massachusetts, USA

[2]Broad Institute of Harvard and MIT, Cambridge, Massachusetts, USA

[3]IBM Research, Yorktown Heights, New York, USA

[4]Candiolo Cancer Institute, FPO-IRCCS, Candiolo (TO), Italy

[5]Department of Oncology, University of Torino, Candiolo (TO)

[6]Dana-Farber Cancer Institute, Boston, Massachusetts, USA

[7]Howard Hughes Medical Institute, Boston, Massachusetts, USA

[8]Massachusetts General Hospital Department of Pathology, Boston, Massachusetts, USA

Abstract

During cancer therapy, tumor heterogeneity can drive the evolution of multiple tumor subclones harboring unique resistance mechanisms in an individual patient[1–3]. Prior case reports and small

Users may view, print, copy, and download text and data-mine the content in such documents, for the purposes of academic research, subject always to the full Conditions of use:http://www.nature.com/authors/editorial_policies/license.html#terms

To whom correspondence should be addressed: Dr. Gad Getz, Broad Institute of Harvard and MIT, 415 Main St., Cambridge, MA, 02142, Phone: 617-714-7471, gadgetz@broadinstitute.org, Dr. Ryan B. Corcoran, Massachusetts General Hospital Cancer Center, 149 13th St., 7th floor, Boston, MA 02129, Phone: 617-726-8599, Fax: 617-724-9648, rbcorcoran@partners.org.

*Denotes equal contribution

Author Contributions

A.R.P., L.G., D.J., R.B.C., I.L., and G.G. conceived of the study; A.R.P., L.G., E.E.V.S., B.N., H.A.S., I.D.-G., M.H.-R., D.D.-S., D.T.T., F.F.d.l.C., A.J.I., I.J.F., G.S., A.B., C.L., F.U., K.R., L.P., I.L., L.E., D.L., E.E.M., and F.A. performed data analysis; A.R.P., L.G., D.D.-S., D.T.T., A.J.I., D.J., R.B.C., G.S., A.B., I.L., and G.G. supervised the data analysis; A.R.P., L.G., E.E.V.S., D.J., R.B.C., C.L., F.U., K.R., L.P., I.L., L.E., D.L., E.E.M., and G.G. participated in data interpretation; A.R.P., E.E.V.S., R.B.C., C.L., F.U., K.R., L.P., I.L., L.E., K.S., B.P.D., and G.G. participated in writing of the manuscript; M.H., B.P.D., T.R.G., and V.A.A. suggested manuscript edits; A.R.P., L.G., E.E.V.S., C.J.P., J.N.A., L.S.B., J.W.C., B.G., J.E.M., R.D.N., E.R., D.P.R., C.D.W., E.L.K., J.E.F., D.D.-S., D.T.T., A.X.Z., T.S.H., A.J.I., D.J., R.B.C., M.H., A.W., V.A. performed sample/data collection; funding was obtained by T.R.G., and G.G.; and A.R.P., E.E.V.S., C.J.P., R.B.C., M.H., K.S., A.W., B.P.D., and G.G. participated in project administration.

Author Manuscript Author Manuscript Author Manuscript Author Manuscript

case series have suggested that liquid biopsy (specifically, cell-free DNA (cfDNA)) may better capture the heterogeneity of acquired resistance[4–8]. However, the effectiveness of cfDNA versus standard single-lesion tumor biopsies has not been directly compared in larger scale prospective cohorts of patients following progression on targeted therapy. Here, in a prospective cohort of 42 patients with molecularly-defined gastrointestinal cancers and acquired resistance to targeted therapy, direct comparison of post-progression cfDNA versus tumor biopsy revealed that cfDNA more frequently identified clinically-relevant resistance alterations and multiple resistance mechanisms, detecting resistance alterations not found in the matched tumor biopsy in 78% of cases. Whole-exome sequencing of serial cfDNA, tumor biopsies, and rapid autopsy specimens elucidated substantial geographic and evolutionary differences across lesions. Our data suggest that acquired resistance is frequently characterized by profound tumor heterogeneity, and that the emergence of multiple resistance alterations in an individual patient may represent the “rule” rather than the “exception.” These findings have profound therapeutic implications and highlight the potential advantages of cfDNA over tissue biopsy in the setting of acquired resistance.

Keywords

Acquired resistance; liquid biopsy; cell-free DNA

The inevitable emergence of acquired resistance is a major limitation of current targeted therapies[9]. Several key studies highlight the potential role that tumor heterogeneity plays in the emergence of resistance[3,4,7,10–14]. In acquired resistance, the evolutionary pressure of therapy can drive outgrowth of distinct tumor subclones harboring independent resistance mechanisms in individual patients, within different metastatic lesions or within the same lesion[1,5,7,10,13]. Genomic analysis of standard single-lesion tumor biopsies upon disease progression has been the mainstay of identifying mechanisms of acquired resistance, but recent studies suggest tumor biopsies may vastly under-represent the heterogeneity of resistance in a single patient[5,7,10,15,16]. In particular, analyzing a core biopsy from one region of a single metastatic lesion may fail to detect clinically-relevant resistance mechanisms, leading to mixed responses or failure of subsequent therapy[3,7,17].

Liquid biopsy, specifically, cell-free DNA (cfDNA), may offer advantages for assessing tumor heterogeneity[4,18,19]. Tumor-derived cfDNA, also termed circulating tumor DNA (ctDNA), is shed from tumor cells throughout the body. Therefore, cfDNA analysis can potentially identify multiple concurrent heterogeneous resistance mechanisms in individual patients that single-lesion tumor biopsies may miss[8,20–22]. While case reports and small case series have suggested advantages of cfDNA[4,5,7,23], cfDNA and tumor biopsy have not been directly compared in larger scale prospective patient cohorts following progression on targeted therapy.

Therefore, we evaluated a prospective cohort of molecularly-defined gastrointestinal (GI) cancer patients who developed acquired resistance to targeted therapy. Through a systematic, disease center–wide liquid biopsy program, 42 patients who achieved stable disease or partial response to targeted therapy underwent liquid biopsy. When possible, a matched tumor biopsy at the time of eventual disease progression was obtained (23 patients). Patients

Author Manuscript Author Manuscript Author Manuscript Author Manuscript

encompassed seven molecular subtypes across three tumor types (Supplementary Table 1), offering a general assessment of cfDNA upon acquired resistance. To identify candidate acquired resistance mechanisms, cfDNA isolated from post-progression plasma was analyzed by next-generation sequencing (NGS) to identify emergent alterations not detected in pre-treatment tumor or cfDNA. Targeted NGS was performed in all cases, with parallel whole-exome sequencing (WES) when tumor fraction in cfDNA was sufficient (>5%). Only previously reported and functionally-validated resistance alterations were counted as resistance mechanisms[5,7,8,12,13,15,21–35] (Supplementary Table 2).

Post-progression cfDNA identified at least one previously validated resistance alteration in 32/42 (76%) patients. Notably, 17/32 (53%) of these patients (40% of all) exhibited >1 detectable resistance alteration (range 2–9, median 3 per patient), suggesting frequent and profound tumor heterogeneity associated with acquired resistance (Fig. 1, Supplementary Table 3). In total, 78 clinically-relevant resistance alterations were found in cfDNA across multiple molecularly-defined tumor types receiving various targeted therapies.

To compare the effectiveness of cfDNA versus standard tumor biopsy, we analyzed matched post-progression tumor biopsies from 23 patients by WES and/or targeted NGS and compared to pre-treatment tumor tissue. Tumor biopsy identified resistance alterations less frequently than cfDNA in only 11/23 (48%) patients (Fig. 1, Extended Data Fig. 1), whereas cfDNA identified at least one resistance alteration in 20/23 (87%) patients, and in 76% of all patients. Moreover, multiple resistance alterations were identified in the post-progression biopsy in only 2/23 cases (9%). This contrasts with cfDNA, where 40% of patients harbored multiple resistance alterations, with up to nine alterations in a single patient. Overall, post-progression cfDNA identified additional clinically-relevant resistance alterations not detected in the post-progression tumor biopsies in 18/23 (78%) cases.

Conversely, only 1/23 (4%) post-progression tumor biopsy identified a resistance alteration that was not detected in matched post-progression cfDNA by NGS. In TPS125—a *RAS* wild type colorectal cancer (CRC) patient treated with the anti-EGFR antibody cetuximab—an $EGFR^{K489E}$ mutation, affecting its antibody-binding domain, was identified in a post-progression biopsy at 11.9% allele frequency (cancer cell fraction: 78%). $EGFR^{K489E}$ was not detected by clinical NGS in post-progression cfDNA, but was detected upon re-analysis using high-sensitivity ddPCR at 0.53% allele frequency (near the lower detection limit of clinical NGS assays for cfDNA, Supplementary Table 4). Thus, some low-level resistance alterations in rare tumor subclones may exist below the detection level in cfDNA with current technologies. Still, remarkably, every resistance alteration identified in a post-progression tumor biopsy was also detectable in matched cfDNA, suggesting that, while possible, missing resistance alterations by cfDNA analysis may be infrequent.

Interestingly, five cases with post-progression tumor biopsies had subsequent tumor specimens available for analysis, obtained during standard clinical care or through an institutional rapid autopsy program. In all cases, additional resistance mechanisms detected in post-progression cfDNA were later found in distinct metastatic lesions (Extended Data Fig. 2).

Author Manuscript Author Manuscript Author Manuscript Author Manuscript

TPS037, a 53-year-old male with metastatic *BRAF*^{V600E} CRC, was treated with a combination of EGFR, BRAF, and PI3Kα inhibitors (cetuximab, encorafenib, and alpelisib;) for 16 months before tumor progression[15]. Biopsy of a progressing liver lesion revealed the original *BRAF*^{V600E} mutation and an emergent *KRAS*^{G12S} mutation (Fig. 2a). Post-progression cfDNA analysis by clinical NGS (Guardant360®) showed not only the original *BRAF*^{V600E} and the emergent *KRAS*^{G12S} mutations, but also *NRAS*^{Q61R} and low-level *EGFR* amplification—all known resistance mechanisms in *BRAF*^{V600E} CRC[15,24,32]. Subsequently, the patient underwent: (1) resection of a brain metastasis; (2) a second protocol-related liver biopsy; and (3) biopsy of a symptomatic subcutaneous soft-tissue lesion.

To better understand the subclonal architecture of resistance, post-progression tumor specimens and cfDNA were analyzed by WES. Consistent with prior reports, the original, likely clonal, *BRAF*^{V600E} mutation persisted in all specimens (Fig. 2a). *KRAS*^{G12S} was detected by WES in both liver biopsies, but not in the brain or soft-tissue metastases. Interestingly, the brain lesion harbored an *EGFR* amplification not detected in any other tumor specimen but detected at low level in cfDNA by clinical NGS. High-sensitivity ddPCR analysis of each tumor specimen also identified *KRAS*^{G12S} (allele frequency 0.17%) in the subcutaneous lesion and *NRAS*^{Q61R} (allele frequency 3.1%) in one liver biopsy (Supplementary Table 4). Thus, all three resistance alterations identified in cfDNA were identified in at least one of the post-progression tumor samples, though no single biopsy harbored all alterations. The clonal architecture and phylogenetic relationship of the four post-progression tumor biopsies and cfDNA by WES (Figs. 2b,c; Supplementary Table 5) showed shared clonal (truncal), private clonal, and subclonal alterations present across various samples. Consistent with the detectability in cfDNA of all resistance alterations present in the individual tumor biopsies, each clonal and the majority of subclonal mutation clusters found in different tumor biopsies were represented (at clonal or subclonal frequencies) in cfDNA, again highlighting the ability of cfDNA to capture heterogeneous molecular alterations present in distinct tumor lesions in an individual patient.

Similarly, TPS177, a 58-year-old woman with metastatic gastric adenocarcinoma harboring a fusion between *CD44* (exons 1–8) and *FGFR2* (exons 3–18), received the FGFR inhibitor Debio1347 (), achieving stable disease for four months before progression. Serial cfDNA analysis (Fig. 3a, Supplementary Table 4) revealed an initial decrease in the abundance of a clonal founder mutation *RHOA*^{Y42C}—representative of overall tumor burden—which rebounded rapidly upon progression and was accompanied by the emergence of four *FGFR2* mutations: (1) *FGFR2*^{V564L}, affecting the gatekeeper residue in the inhibitor binding site, (2) *FGFR2*^{L617V} and (3) *FGFR2*^{E565A}—all known mechanisms of resistance to FGFR inhibition, and (4) *FGFR2*^{S780L}, which resides outside the kinase domain and may not represent a true resistance alteration[7]. As high-level *FGFR2*-fusion amplification was present (>50–150 copies), the existence of a potential passenger mutation would not be surprising. The patient underwent biopsy of a progressing paraaortic lymph node, but unfortunately expired due to disease complications. Rapid autopsy yielded 17 tumor lesions from various anatomic sites.

Author Manuscript Author Manuscript Author Manuscript Author Manuscript

We analyzed WES data from pre-treatment and post-progression cfDNA, post-progression biopsy, and 17 autopsy specimens (Figs. 3b–d; Supplementary Table 5), and studied the clones and their phylogenetic structure with PhylogicNDT[36]. Interestingly, *FGFR2*^{V564L} (detected in post-progression cfDNA) was found predominantly in liver metastases, whereas *FGFR2*^{L617V} (also in progression cfDNA) had an anti-correlated pattern, predominantly detected in other metastatic sites, suggesting these alterations confer resistance in different cell populations. *FGFR2*^{E565A}, detected in cfDNA, was identified at low level in a single liver lesion (D). Interestingly, autopsy specimens from the stomach (M/N/O), the primary tumor site, harbored only low levels of either resistance alteration. WES and RNAseq of stomach lesions also did not detect clear evidence of the *CD44–FGFR2* fusion and showed markedly reduced *FGFR2* expression levels and local copy number relative to other lesions (Fig. 3c). Phylogenetic analysis suggested that subclones present in these lesions likely represent early ancestors (Fig. 3b, **upper right branch**) that may have existed prior to development of the *CD44–FGFR2* fusion–containing clone that later seeded the majority of metastases. Thus, in these stomach lesions, resistance to FGFR inhibition may have occurred primarily due to outgrowth of an early fusion-negative clone. *FGFR2* fusion as a late event is consistent with the biology of gastric cancer, where RTK amplifications (e.g., *ERBB2* or *MET)* can occur as late events, leading to outgrowth of non-amplified clones during targeted therapy[30,37–39]. However, the presence of *FGFR2* resistance alterations at low levels suggests that some fusion-positive subclones may have remained in these lesions, but at levels too low for detection by WES or RNAseq. Overall, all three *FGFR2* mutations and the majority of private alterations present in individual tumors were detected in post-progression cfDNA (Figs. 3c,d).

Our data illustrate that acquired resistance to targeted therapy in GI cancers is highly heterogeneous, often with multiple resistance alterations per patient, and that liquid biopsy can effectively detect multiple resistance alterations residing concurrently in distinct tumor subclones and different metastatic lesions. Remarkably, a resistance alteration detected in a tumor biopsy but not in the matched cfDNA by clinical NGS occurred in only 1/23 cases. However, this alteration indeed existed in cfDNA and was detected using a higher sensitivity method. Thus, while cfDNA analysis may miss rare tumor subclones, our study suggests effective representation of alterations from multiple lesions in cfDNA. However, cfDNA detection effectiveness may differ by tumor type, metastatic site, or in tumors with low rates of ctDNA shedding.

This study has several potential limitations. Although it represents one of the largest direct comparisons of post-progression cfDNA and matched tumor biopsy to date, overall patient numbers remain limited. Thus, additional studies may further define the degree of heterogeneity upon acquired resistance and its relevance beyond gastrointestinal cancers. Additionally, in some cases, multiple biopsies and rapid autopsy confirmed that the multiple resistance alterations detected in cfDNA were derived from specific tumor lesions, but multiple tumor specimens were not available for most patients. However, in a comparator cohort of patients with similar clinical characteristics (Supplementary Table 6) with cfDNA analysis after progression on standard cytotoxic chemotherapy alone, without targeted therapy, we did not observe emergence of any of the clinically-relevant resistance alterations

Author Manuscript Author Manuscript Author Manuscript Author Manuscript

listed in Supplementary Table 2, suggesting that resistance alterations detected in cfDNA in our study represent tumor-derived alterations emerging under selective pressure from targeted therapy. Finally, cfDNA analysis is unlikely to detect non-genetic resistance mechanisms; in 24% of cases, no resistance mechanisms were detected by cfDNA or tumor biopsy. Although analysis of alterations in these patients revealed shared patterns of copy-number alterations with tumors having a known mechanism, a clear genomic driver of resistance could not be identified (Extended Data Fig. 3, Supplementary Table 7). Thus, tumor biopsy will still be key in assessing acquired resistance, particularly for novel or non-genetic resistance mechanisms.

In conclusion, direct comparison of cfDNA versus tumor biopsy illustrates how single-lesion tumor biopsies in the setting of acquired resistance frequently fail to identify the presence of multiple clinically-relevant resistance mechanisms, with cfDNA identifying additional concurrent resistance mechanisms in 78% of cases. Thus, our data suggest that single-lesion tumor biopsy alone is inadequate for characterizing acquired resistance, and that cfDNA regularly identifies heterogeneous clinically-relevant resistance alterations critical to the selection of subsequent therapy. This finding has important clinical implications: a treatment strategy aiming to overcome resistance will need to address the fact that a patient likely harbors multiple subclones with different resistance mechanisms. A recent study demonstrated the effectiveness of cfDNA analysis for selecting initial molecularly-directed therapy[40]. Similarly, our results support that clinical incorporation of post-progression liquid biopsy may have a valuable role in efforts to assess and overcome acquired resistance.

ONLINE METHODS

Patients and specimen collection

All biopsies, tumor specimens, and peripheral blood draws for plasma isolation were collected in accordance with Institutional Review Board–approved protocols, to which patients provided written informed consent, and all studies were conducted in accordance with the Declaration of Helsinki. Patients provided informed written consent for blood and tissue collection and for genomic analysis of these specimens. Through a systematic liquid biopsy program in the Center for Gastrointestinal Cancers at the Massachusetts General Hospital Cancer Center, plasma collection for post-progression cfDNA analysis was attempted for all patients receiving targeted therapy for molecularly-defined GI cancer subtypes who achieved radiologic response or stable disease between September 2014 and March 2018. In total, 42 patients were studied. Peripheral blood was collected in two 10 mL Streck tubes upon disease progression for cfDNA analysis. When possible, post-progression tumor biopsies (solid and blood) were obtained in parallel at the time of progression, which were obtained in 23/42 patients. Pre-treatment tumor tissue was available for analysis in all 42 cases, and pre-treatment cfDNA in 19 cases. Rapid autopsies were performed within the first 3 hours postmortem. Targeted exome sequencing on clinical tissue specimens using a Clinical Laboratory Improvement Amendment (CLIA)–certified clinical NGS assay was performed in the Department of Molecular Pathology at the Massachusetts General Hospital. A subset of patients for whom tumor and cfDNA specimens harbored sufficient tumor DNA content were analyzed by WES, as described below. Imaging studies, including CT and MRI

Author Manuscript Author Manuscript Author Manuscript Author Manuscript

scans, were obtained as part of routine clinical care. A comparator cohort of consecutive GI cancer patients who did not receive targeted therapy, who underwent clinical NGS analysis of cfDNA (Guardant360®) as part of routine clinical care after disease progression on standard cytotoxic chemotherapy (including patients who received anti-angiogenic therapy, such as bevacizumab and two patients with no prior therapy), and who had comprehensive baseline clinical tumor NGS testing and provided informed written consent as above were also evaluated.

cfDNA isolation and analysis

Whole blood was collected by routine phlebotomy in two 10 mL Streck tubes. Plasma was separated within 1–4 days of collection through two different centrifugation steps (the first at room temperature or 10 minutes at 1600 x g and the second at 3000 x g for the same time and temperature). Plasma was stored at −80°C until cfDNA extraction. cfDNA was extracted from plasma using the QIAamp Circulating Nucleic Acid Kit (QIAGEN) according to the manufacturer's instructions.

Clinical NGS analysis of cfDNA was conducted using the Guardant360® assay. Peripheral blood was collected in two 10 mL Streck tubes and shipped for centralized processing and testing (Guardant Health, Redwood City, CA) in accordance with standard clinical testing procedures. Sequencing libraries were prepared from up to 30 ng cfDNA with custom in-line barcode molecular tagging, and complete sequencing at 15,000 × read depth of the critical exons in a targeted panel of 70+ genes was performed at a Clinical Laboratory Improvement Amendments (CLIA)–certified, College of American Pathologists–accredited laboratory (Guardant Health)[41]. Targeted NGS of cfDNA for 226 cancer-related genes using the IRCC-Target panel was performed as previously reported[7,8]. To identify candidate mechanisms of acquired resistance, in each case cfDNA sequencing data from plasma obtained post-progression was compared to sequencing data from pre-treatment tumor or cfDNA as available to identify emergent alterations not detected in the pre-treatment specimens.

For droplet digital PCR (ddPCR) experiments, DNA template (8 to 10 μL) was added to 10 μL of ddPCR Supermix for Probes (Bio-Rad) and 2 μL of the custom primer/probe mixture. This reaction mix was added to a DG8 cartridge together with 60 μL of Droplet Generation Oil for Probes (Bio-Rad) and used for droplet generation. Droplets were then transferred to a 96-well plate (Eppendorf) and then thermal cycled with the following conditions: 5 minutes at 95°C, 40 cycles of 94°C for 30 seconds, 55°C for 1 minute followed by 98°C for 10 minutes (Ramp Rate 2°C/sec). Droplets were analyzed with the QX200 Droplet Reader (Bio-Rad) for fluorescent measurement of FAM and HEX probes. Gating was performed based on positive and negative controls, and mutant populations were identified. The ddPCR data were analyzed with QuantaSoft analysis software (Bio-Rad) to obtain Fractional Abundance of the mutant DNA alleles in the wild-type/normal background. The quantification of the target molecule was presented as the number of total copies (mutant plus wild-type) per sample in each reaction. Allelic fraction is calculated as follows: AF % = $(N_{mut}/(N_{mut}+N_{wt}))*100$), where N_{mut} is the number of mutant alleles and N_{wt} is the number of wild-type alleles per reaction. A minimum coverage depth of 300X was achieved for each analysis. ddPCR analysis of normal control plasma DNA (from cell lines) and no DNA

Author Manuscript Author Manuscript Author Manuscript Author Manuscript

template controls were always included. Probe and primer sequences are available upon request.

Whole exome sequencing data

For whole-exome sequencing (WES), the AllPrep DNA/RNA Mini Kit (Qiagen, Hilden, Germany) was used for dual extraction of both genomic DNA and RNA. DNA was quantified in triplicate using a standardized PicoGreen® dsDNA Quantitation Reagent (Invitrogen, Carlsbad, CA) assay. The quality control identification check was performed using fingerprint genotyping of 95 common SNPs by Fluidigm Genotyping (Fluidigm, San Francisco, CA). Library construction from double stranded DNA was performed using the KAPA Library Prep kit, with palindromic forked adapters from Integrated DNA Technologies. Libraries were pooled prior to hybridization. Hybridization and capture were performed using the relevant components of Illumina's Rapid Capture Enrichment Kit, with a 37Mb target. All library construction, hybridization and capture steps were automated on the Agilent Bravo liquid handling system. After post-capture enrichment, library pools were denatured using 0.1N NaOH on the Hamilton Starlet. Cluster amplification of DNA libraries was performed according to the manufacturer's protocol (Illumina) using HiSeq 4000 exclusion amplification chemistry and HiSeq 4000 flowcells. Flowcells were sequenced utilizing Sequencing-by-Synthesis chemistry for HiSeq 4000 flowcells. The flowcells were then analyzed using RTA v.2.7.3 or later. Each pool of whole exome libraries was sequenced on paired 76 cycle runs with two 8 cycle index reads across the number of lanes needed to meet coverage for all libraries in the pool.

Phylogenetic analysis of multiple samples from the same patient

WES data were analyzed on the FireCloud cloud-based analysis platform (https://portal.firecloud.org/). Somatic mutations for each tumor/normal pair were detected using the Cancer Genome Analysis WES Characterization Pipeline available on FireCloud. The Characterization Pipeline includes multiple steps, including: MuTect[42] for detection of somatic single nucleotide variants (SSNVs), Strelka[43] for detecting small insertions and deletions (INDELs), deTiN[44] estimates potential tumor-in-normal (TiN) contamination, ContEst[45] for detecting cross-patient contamination, AllelicCapSeg[46] for assessing allele-specific copy-number alterations, and ABSOLUTE[46] for estimating tumor purity, ploidy, absolute allelic copy-number and cancer cell fractions (CCFs). The data for this study consisted of multiple samples collected from each patient (pre- and post-treatment) as well as autopsy samples. Phylogenetic analysis, subclonal reconstruction and tree building was done with the PhylogicNDT package[36].

Tumor clustering based on patterns of commonly acquired alterations

To better characterize patients with an unknown mechanism of resistance, we wanted to identify groups of patients that share similar patterns of alterations that were acquired between the pre-treatment and post-progression samples. We define, for each patient with pre- and post-treatment samples, a set of features that reflect the changes in their somatic alterations between the pre-treatment and post-progression samples, which we call δ (Extended Data Fig. 3a). We focused the analysis on either a list of 609 known cancer genes (Cancer Gene Census, downloaded Oct 2017) or a set of 5,144 genesets (MSigDB class

Author Manuscript Author Manuscript Author Manuscript Author Manuscript

c2.cp and c5.bp, v6 with at most 200 genes). We considered both point mutations (SSNVs or INDELs) and somatic copy-number alterations. When analyzing point mutations, we set $\delta_{gene}=1$ to reflect a significant change in CCF, i.e., if the change in CCF of the mutation in the gene was at least 2 standard deviations above the mean CCF change across all mutations and the post-progression sample had a CCF>0.2. Similarly, when analyzing copy-number, we set $\delta_{gene}=1$ to reflect a significant copy-number change, i.e., if the change was greater than 2 standard deviations above or below the mean change in copy-number levels, and the gene was either amplified (copy-number level>4) or deleted (copy-number level <1) in the post-progression sample, respectively. To study genesets, we set $\delta_{geneset}$ to reflect the fraction of genes in the geneset that have a significant change in either copy-number or mutation CCF, accounting for the size of the geneset and the total number of significant genes in the patient.

Next, in order to find groups of patients that have similar changes in their somatic alterations, we applied the BiMax biclustering algorithm[47] to each of the four δ matrices: $\delta^{\text{copy}-\text{number}}_{\text{cancer gene}}$, $\delta^{\text{mutation}}_{\text{geneset}}$, $\delta^{\text{copy}-\text{number}}_{\text{geneset}}$, and $\delta^{\text{copy}-\text{number and mutation}}_{\text{geneset}}$. This analysis yielded between 3 and 11 biclusters (Extended Data Figs. 3b–e). To evaluate the significance of the resulting biclusters, we used a two-sided t-test to compare the mean size of biclusters observed in the matrix against results from n=10000 permuted matrices, where the values of the matrix were shuffled and biclustered.

Data availability

Sequencing data from WES and RNA-seq will be available in dbGaP in accession number phs001853.v1.p1.

Extended Data

Author Manuscript Author Manuscript Author Manuscript Author Manuscript

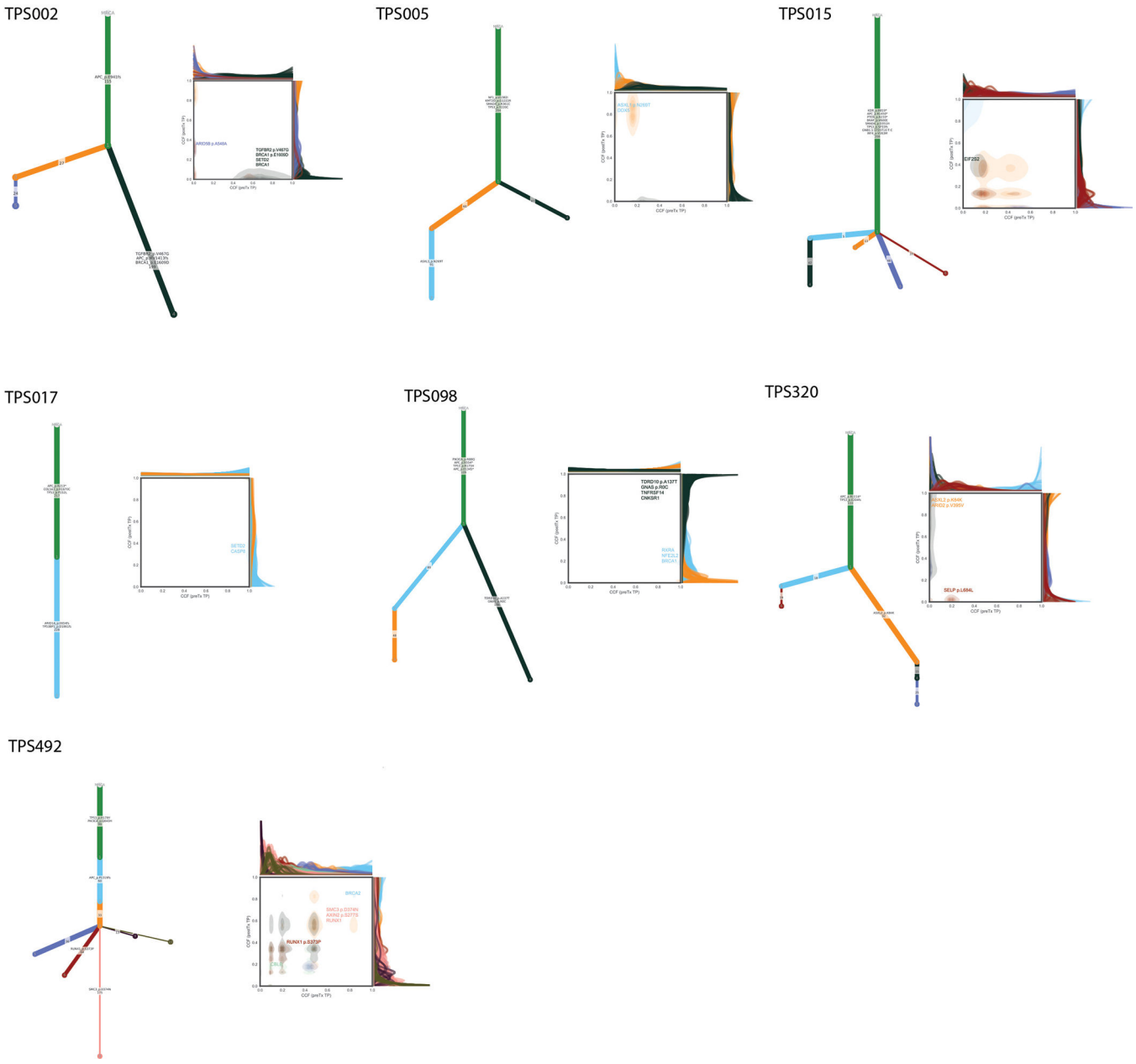

Extended Data Figure 1: Phylogenetic trees for paired tumor biopsies

Phylogenetic trees for patients with WES for pre- and post-treatment samples. The number of somatic alterations assigned to each cluster and detected events in known cancer genes appear on the branches. A 2-D plot showing the cancer cell fraction distribution of subclones in the pre- and post-treatment samples. Events in known cancer are shown next to their subclonal cluster.

Author Manuscript Author Manuscript Author Manuscript Author Manuscript

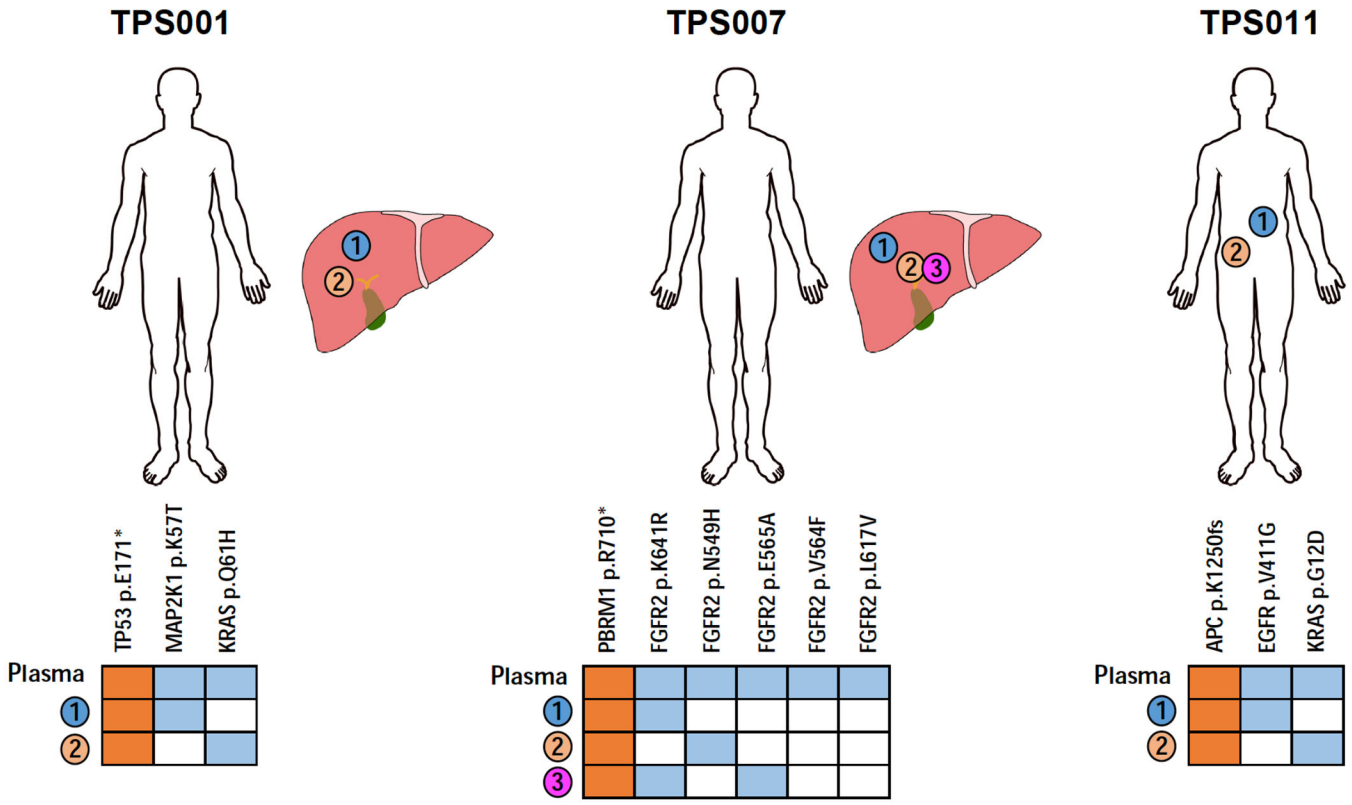

Extended Data Figure 2: Patients with multiple post-progression tumor biopsies.

Three of five patients with multiple post-progression tumor biopsies are shown. The other two patients (TPS037 and TPS177) are shown in Figures 2 and 3, respectively. For each patient, the location of each tumor biopsy and the resistance alterations (blue) and truncal alterations (orange) detected in cfDNA and in each tumor specimen are shown. TPS001 is a *RAS* wild type colorectal cancer patient who developed resistance to an anti-EGFR antibody[8]. Biopsy of one liver lesion revealed an activating *MEK1* (*MAP2K1*) mutation, and biopsy of a second liver lesion identified a *KRAS* mutation. Both resistance alterations were detected in post-progression cfDNA. TPS007 is an *FGFR2*-fusion positive cholangiocarcinoma patient who developed resistance to an FGFR inhibitor[5]. Five *FGFR2* resistance mutations were identified in post-progression cfDNA, and three of these alterations were identified in distinct liver lesions harvested through a rapid autopsy program, with one lesion harboring two *FGFR2* alterations. TPS011 is a RAS WT colorectal cancer patient who developed resistance to an anti-EGFR antibody. A recurrent colon tumor harbored a *KRAS* mutation, and an *EGFR* extracellular domain mutation--known to interfere with antibody binding--was identified in an ovarian metastasis, whereas both alterations were detected in cfDNA. Importantly, in all patients, individual resistance mechanisms emerging in distinct metastatic lesions were detectable in cfDNA.

Author Manuscript Author Manuscript Author Manuscript Author Manuscript

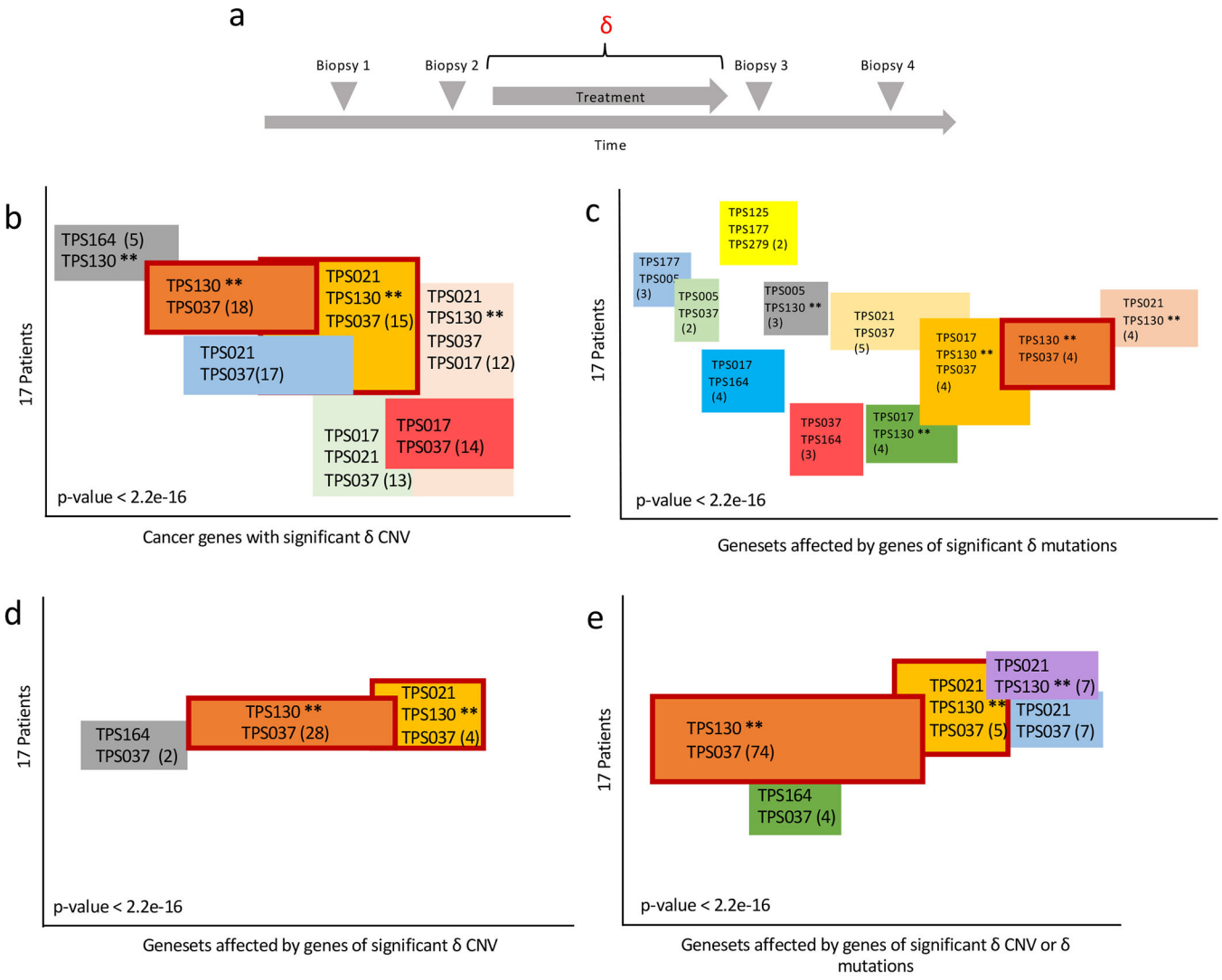

Extended Data Figure 3: Biclusters of patients based on similar changes (δ) in somatic alteration.

Biclustering of four δ matrices reflecting changes in cancer cell fraction of mutations or copy-number in known cancer genes or genesets yielded significant biclusters (all empirical p-values<0.0001; Online Methods). The biclusters from all four δ matrices included at least one bicluster with patient TPS130, a patient with an unknown mechanism of resistance. Patient TPS130 consistently biclustered together with TPS021 and TPS037, patients with known mechanisms of resistance, across all matrices, highlighting the possibility that additional genomic alterations contribute to resistance beyond the identified resistance alterations. (**a**) The change in somatic alterations, δ, is calculated based on WES data of the samples closest to the start and end of therapy. We biclustered four δ matrices: $\delta_{cancer\ gene}^{copy-number}$, $\delta_{geneset}^{mutation}$, $\delta_{geneset}^{copy-number}$, and $\delta_{geneset}^{copy-number\ and\ mutation}$ and assessed their significance by comparing the size of biclustersagainst n=10000 permuted matrices with a two-sided t-test (Online Methods). (**b-e**) Illustration of the biclustering results (using

Author Manuscript Author Manuscript Author Manuscript Author Manuscript

BiMax) of the four δ matrices (biclusters listed in Supplementary Table 6). Outlined in red are biclusters containing TPS130 observed in all four δ matrices.

Supplementary Material

Refer to Web version on PubMed Central for supplementary material.

Acknowledgments

Grant Support

The work is partially supported by NIH/NCI Gastrointestinal Cancer SPORE P50 CA127003, R01CA208437, K08CA166510, U54CA224068, a Damon Runyon Clinical Investigator Award, and a Stand Up To Cancer Colorectal Dream Team Translational Research Grant (grant number SU2C-AACR-DT22-17; to R.B.C.). Research grants are administered by the American Association of Cancer Research, the scientific partners of SU2C. The work is partially supported by the Broad/IBM Cancer Resistance Research Project (G.G, L.P), and the Susan Eid Tumor Heterogeneity Initiative (D.J.). A.B. was supported by European Community's Seventh Framework Programme under grant agreement no. 602901 MErCuRIC; H2020 grant agreement no. 635342-2 MoTriColor; IMI contract n. 115749 CANCER-ID; AIRC IG 2015 n. 16788; FONDAZIONE AIRC under 5 per Mille 2018 - ID. 21091 program; AIRC IG 2018 - ID. 21923 project; AIRC-CRUK-FC AECC Accelerator Award contract 22795; Progetto NET-2011-02352137 Ministero della Salute; Fondazione Piemontese per la Ricerca sul Cancro-ONLUS 5 per mille 2014 e 2015 Ministero della Salute. G.S. was funded by Roche per la Ricerca grant 2017 and AIRC three years fellowship 2017.

Disclosure of Potential Conflicts of Interest

A.R.P is a consultant/advisory board member for Puretech, Driver, Foundation Medicine and Eisai; and has institutional research funding from Array, Plexxikon, Guardant, BMS, MacroGenics, Genentech, Novartis, OncoMed, and Tolero. L.G. is a consultant/advisory board member for Debiopharm, H3 Biomedicine, and Pieris Pharmaceuticals and a Steering Committee Member for Agios Pharmaceuticals, Taiho Pharmaceuticals, and Debiopharm. E.R. is advisory board member/consultant for Helsinn, Heron, BASF, American Imaging Management, Napo, Imuneering and Vector Oncology. D.P.R. serves on advisory boards for MPM Capital, Gritstone Oncology, Oncorus, and TCR2; has equity in MPM Capital and Acworth Pharmaceuticals; serves as author for Johns Hopkins University Press, UpToDate, McGraw Hill. C.W is a consultant for Celgene. J.E.F. is an employee at Novartis; had served as advisory board member/consultant for Merrimack, and N-one-One; research funding from Novartis, Roche/Genentech, Agios, Takeda, Sanofi, Celgene and Exelixis; travel support from Roche/Genentech. E.L.K. is an employee of Novartis. M.H.-R. is an employee of Forma Therapeutics. D.T.T. is a consultant/advisory board member for Merrimack Pharmaceuticals, Roche Ventana, EMD Millipore-Sigma. D.T.T. is founder and has equity in PanTher Therapeutics. D.T.T. receives research funding from ACD-Biotechne. A.X.Z is a consultant/advisor for AstraZeneca, Bayer, Bristol-Myers Squibb, Eisai, Eli Lilly, Exelixis, Merck, Novartis, and Roche/Genentech; research funding from Bayer, Bristol-Myers Squibb, Eli Lilly, Merck, and Novartis. T.S.H. is consultant/advisory board member for Merck and EMD Serono; research support from Taiho, Astra Zeneca, Bristol Myers Squibb, Mobetron, and Ipsen. A.J.I. is a consultant for DebioPharm, Chugai, and Roche; research support from Sanofi and has equity in ArcherDx. T.G. is a consultant/advisor for Foundation Medicine, GlaxoSmithKline, Sherlock Biosciences, FORMA Therapeutics. R.B.C. is a consultant/advisory board member for Amgen, Array Biopharma, Astex Pharmaceuticals, Avidity Biosciences, BMS, C4 Therapeutics, Chugai, Elicio, Fog Pharma, Fount Therapeutics, Genentech, LOXO, Merrimack, N-of-one, Novartis, nRichDx, Revolution Medicines, Roche, Roivant, Shionogi, Shire, Spectrum Pharmaceuticals, Symphogen, Taiho, and Warp Drive Bio; holds equity in Avidity Biosciences, C4 Therapeutics, Fount Therapeutics, nRichDx, and Revolution Medicines; and has received research funding from Asana, AstraZeneca, and Sanofi. T.R.G. is or has been a recent paid advisor to GlaxoSmithKline, Foundation Medicine, Sherlock Biosciences, and holds equity in Sherlock Biosciences and FORMA Therapeutics. D.J. is an advisor/consultant for Novartis, Genentech, Eisai, Ipsen, EMD Serono; receives research support from Novartis, Genentech, Eisai, EMD Serono, Takeda, Celgene, and Placon. G.G receives research funds from IBM and Pharmacyclics. G.G. is an inventor on patent applications related to MuTect and ABSOLUTE, POLYSOLVER as well as others. K.R., F.U., C.L. and L.P. are listed as co-inventors on a patent application currently pending review at the USPTO. I.L. L.E., D.L., E.E.V.S., E.E.M., M.H., K.S., C.J.P, A.W., B.P.D, F.F.d.l.C., I.J.F., B.N., H.A.S., J.N.A., L.S.B., J.W.C., B.G., J.E.M., R.D.N., F.A., I.D.-G., D.D.-S., V.A.A. have no disclosures.

Author Manuscript Author Manuscript Author Manuscript Author Manuscript

REFERENCES

1. Burrell RA & Swanton C Tumour heterogeneity and the evolution of polyclonal drug resistance. Mol. Oncol 8, 1095–1111 (2014). [PubMed: 25087573]
2. Gerlinger M, et al. Genomic architecture and evolution of clear cell renal cell carcinomas defined by multiregion sequencing. Nat. Genet 46, 225–233 (2014). [PubMed: 24487277]
3. McGranahan N & Swanton C Biological and therapeutic impact of intratumor heterogeneity in cancer evolution. Cancer Cell 27, 15–26 (2015). [PubMed: 25584892]
4. Bettegowda C, et al. Detection of circulating tumor DNA in early- and late-stage human malignancies. Sci. Transl. Med 6, 224ra224 (2014).
5. Goyal L, et al. Polyclonal Secondary Mutations Drive Acquired Resistance to FGFR Inhibition in Patients with FGFR2 Fusion-Positive Cholangiocarcinoma. Cancer Discov. 7, 252–263 (2017). [PubMed: 28034880]
6. Piotrowska Z, et al. Heterogeneity Underlies the Emergence of EGFRT790 Wild-Type Clones Following Treatment of T790M-Positive Cancers with a Third-Generation EGFR Inhibitor. Cancer Discov. 5, 713–722 (2015). [PubMed: 25934077]
7. Russo M, et al. Tumor Heterogeneity and Lesion-Specific Response to Targeted Therapy in Colorectal Cancer. Cancer Discov. 6, 147–153 (2016). [PubMed: 26644315]
8. Siravegna G, et al. Clonal evolution and resistance to EGFR blockade in the blood of colorectal cancer patients. Nat. Med 21, 827 (2015).
9. Garraway LA & Jänne PA Circumventing cancer drug resistance in the era of personalized medicine. Cancer Discov. 2, 214–226 (2012). [PubMed: 22585993]
10. Gerlinger M, et al. Intratumor heterogeneity and branched evolution revealed by multiregion sequencing. N. Engl. J. Med 366, 883–892 (2012). [PubMed: 22397650]
11. Jamal-Hanjani M, et al. Tracking the Evolution of Non-Small-Cell Lung Cancer. N. Engl. J. Med 376, 2109–2121 (2017). [PubMed: 28445112]
12. Misale S, Di Nicolantonio F, Sartore-Bianchi A, Siena S & Bardelli A Resistance to anti-EGFR therapy in colorectal cancer: from heterogeneity to convergent evolution. Cancer Discov. 4, 1269–1280 (2014). [PubMed: 25293556]
13. Misale S, et al. Emergence of KRAS mutations and acquired resistance to anti-EGFR therapy in colorectal cancer. Nature 486, 532–536 (2012). [PubMed: 22722830]
14. Turajlic S, et al. Deterministic Evolutionary Trajectories Influence Primary Tumor Growth: TRACERx Renal. Cell 173, 595–610.e511 (2018). [PubMed: 29656894]
15. Hazar-Rethinam M, et al. Convergent Therapeutic Strategies to Overcome the Heterogeneity of Acquired Resistance in BRAFV600E Colorectal Cancer. Cancer Discov. 8, 417–427 (2018). [PubMed: 29431697]
16. Morelli MP, et al. Characterizing the patterns of clonal selection in circulating tumor DNA from patients with colorectal cancer refractory to anti-EGFR treatment. Ann. Oncol 26, 731–736 (2015). [PubMed: 25628445]
17. Piotrowska Z, et al. Heterogeneity and Coexistence of T790M and T790 Wild-Type Resistant Subclones Drive Mixed Response to Third-Generation Epidermal Growth Factor Receptor Inhibitors in Lung Cancer. JCO Precis Oncol 2018(2018).
18. Blakely CM, et al. Evolution and clinical impact of co-occurring genetic alterations in advanced-stage EGFR-mutant lung cancers. Nat. Genet 49, 1693–1704 (2017). [PubMed: 29106415]
19. Haber DA & Velculescu VE Blood-based analyses of cancer: circulating tumor cells and circulating tumor DNA. Cancer Discov. 4, 650–661 (2014). [PubMed: 24801577]
20. Chabon JJ, et al. Circulating tumour DNA profiling reveals heterogeneity of EGFR inhibitor resistance mechanisms in lung cancer patients. Nat. Commun 7, 11815 (2016). [PubMed: 27283993]
21. Diaz LA Jr., et al. The molecular evolution of acquired resistance to targeted EGFR blockade in colorectal cancers. Nature 486, 537–540 (2012). [PubMed: 22722843]
22. Strickler JH, et al. Genomic Landscape of Cell-Free DNA in Patients with Colorectal Cancer. Cancer Discov. 8, 164–173 (2018). [PubMed: 29196463]

Author Manuscript Author Manuscript Author Manuscript Author Manuscript

23. Thierry AR, et al. Circulating DNA Demonstrates Convergent Evolution and Common Resistance Mechanisms during Treatment of Colorectal Cancer. Clin Cancer Res 23, 4578–4591 (2017). [PubMed: 28400427]
24. Ahronian LG, et al. Clinical Acquired Resistance to RAF Inhibitor Combinations in BRAF-Mutant Colorectal Cancer through MAPK Pathway Alterations. Cancer Discov. 5, 358–367 (2015). [PubMed: 25673644]
25. Arena S, et al. MM-151 overcomes acquired resistance to cetuximab and panitumumab in colorectal cancers harboring EGFR extracellular domain mutations. Sci. Transl. Med 8, 324ra314 (2016).
26. Bahcall M, et al. Acquired METD1228V Mutation and Resistance to MET Inhibition in Lung Cancer. Cancer Discov. 6, 1334–1341 (2016). [PubMed: 27694386]
27. Bertotti A, et al. A molecularly annotated platform of patient-derived xenografts ("xenopatients") identifies HER2 as an effective therapeutic target in cetuximab-resistant colorectal cancer. Cancer Discov. 1, 508–523 (2011). [PubMed: 22586653]
28. Bertotti A, et al. The genomic landscape of response to EGFR blockade in colorectal cancer. Nature 526, 263–267 (2015). [PubMed: 26416732]
29. Heist RS, et al. Acquired Resistance to Crizotinib in NSCLC with MET Exon 14 Skipping. J. Thorac. Oncol 11, 1242–1245 (2016). [PubMed: 27343442]
30. Kwak EL, et al. Molecular Heterogeneity and Receptor Coamplification Drive Resistance to Targeted Therapy in MET-Amplified Esophagogastric Cancer. Cancer Discov. 5, 1271–1281 (2015). [PubMed: 26432108]
31. Montagut C, et al. Identification of a mutation in the extracellular domain of the Epidermal Growth Factor Receptor conferring cetuximab resistance in colorectal cancer. Nat. Med 18, 221–223 (2012). [PubMed: 22270724]
32. Oddo D, et al. Molecular Landscape of Acquired Resistance to Targeted Therapy Combinations in BRAF-Mutant Colorectal Cancer. Cancer Res. 76, 4504–4515 (2016). [PubMed: 27312529]
33. Siravegna G, et al. Radiologic and Genomic Evolution of Individual Metastases during HER2 Blockade in Colorectal Cancer. Cancer Cell 34, 148–162.e147 (2018). [PubMed: 29990497]
34. Tan L, et al. Development of covalent inhibitors that can overcome resistance to first-generation FGFR kinase inhibitors. Proc. Natl. Acad. Sci. U. S. A 111, E4869–4877 (2014). [PubMed: 25349422]
35. Yaeger R, et al. Mechanisms of Acquired Resistance to BRAF V600E Inhibition in Colon Cancers Converge on RAF Dimerization and Are Sensitive to Its Inhibition. Cancer Res. 77, 6513–6523 (2017). [PubMed: 28951457]
36. Leshchiner I, et al. Comprehensive analysis of tumour initiation, spatial and temporal progression under multiple lines of treatment. bioRxiv (2018).
37. Janjigian YY, et al. Genetic Predictors of Response to Systemic Therapy in Esophagogastric Cancer. Cancer Discov. 8, 49–58 (2018). [PubMed: 29122777]
38. Kim ST, et al. Impact of genomic alterations on lapatinib treatment outcome and cell-free genomic landscape during HER2 therapy in HER2+ gastric cancer patients. Ann. Oncol 29, 1037–1048 (2018). [PubMed: 29409051]
39. Pectasides E, et al. Genomic Heterogeneity as a Barrier to Precision Medicine in Gastroesophageal Adenocarcinoma. Cancer Discov. 8, 37–48 (2018). [PubMed: 28978556]
40. Rothwell DG, et al. Utility of ctDNA to support patient selection for early phase clinical trials: the TARGET study. Nat Med 25, 738–743 (2019). [PubMed: 31011204]

REFERENCES FOR ONLINE METHODS

41. Lanman RB, et al. Analytical and Clinical Validation of a Digital Sequencing Panel for Quantitative, Highly Accurate Evaluation of Cell-Free Circulating Tumor DNA. PLoS One 10, e0140712 (2015). [PubMed: 26474073]
42. Cibulskis K, et al. Sensitive detection of somatic point mutations in impure and heterogeneous cancer samples. Nat. Biotechnol 31, 213–219 (2013). [PubMed: 23396013]

Author Manuscript Author Manuscript Author Manuscript Author Manuscript

43. Kim S, et al. Strelka2: fast and accurate calling of germline and somatic variants. Nat. Methods 15, 591–594 (2018). [PubMed: 30013048]

44. Taylor-Weiner A, et al. DeTiN: overcoming tumor-in-normal contamination. Nat. Methods 15, 531–534 (2018). [PubMed: 29941871]

45. Cibulskis K, et al. ContEst: estimating cross-contamination of human samples in next-generation sequencing data. Bioinformatics 27, 2601–2602 (2011). [PubMed: 21803805]

46. Carter SL, et al. Absolute quantification of somatic DNA alterations in human cancer. Nat. Biotechnol 30, 413–421 (2012). [PubMed: 22544022]

47. Prelić A, et al. A systematic comparison and evaluation of biclustering methods for gene expression data. Bioinformatics 22, 1122–1129 (2006). [PubMed: 16500941]

Author Manuscript Author Manuscript Author Manuscript Author Manuscript

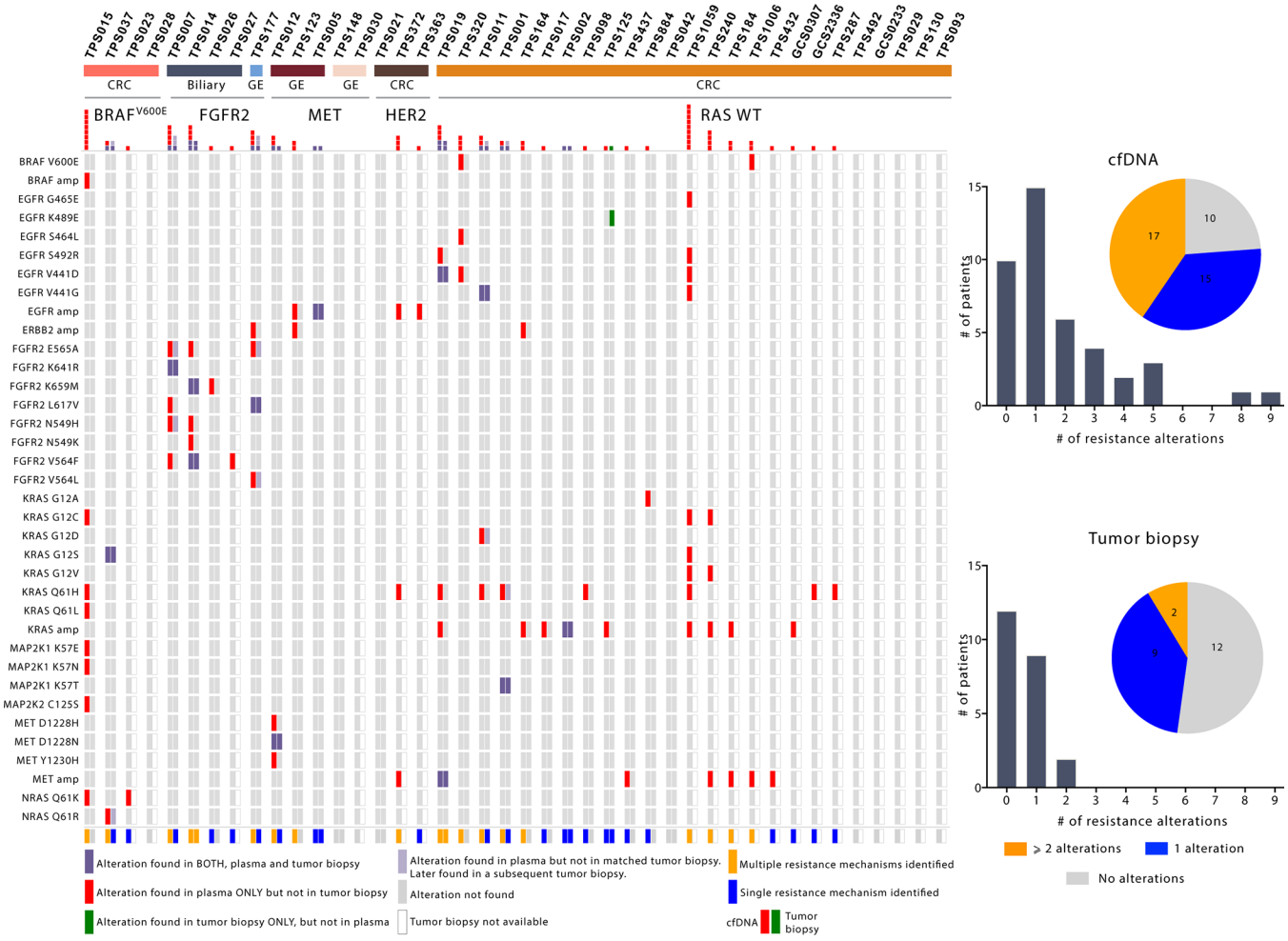

Figure 1: Identification of acquired resistance mechanisms in liquid versus tumor biopsy.

A comparison of specific resistance alterations identified in plasma cfDNA (N=42) versus tumor biopsy (N=23) for each patient. Patients are grouped according to tumor type (N=3) (CRC = colorectal, GE = gastroesophageal, biliary) and molecular subtype (N=5) (*FGFR2* = *FGFR2* fusion, *MET* = *MET* amplification, *HER2* = *HER2* amplification, $BRAF^{V600E}$, *RAS* wild type. Red represents alterations identified in plasma, but not in the tissue biopsies; green represents alterations identified in tissue biopsies, but not in plasma; and purple represents alterations identified in both plasma and tissue biopsies. Pale purple represents alterations identified in plasma that were not detected in the post-progression tissue biopsy but were eventually detected in subsequent tissue biopsies from the same patient. The alterations detected in cfDNA versus tumor biopsy are quantified in a histogram across the top of the panel and are summarized graphically on the right, depicting specifically the percentage of patients with one, more than one, or no experimentally validated resistance alterations identified by cfDNA (top) or tumor biopsy (bottom).

Author Manuscript Author Manuscript Author Manuscript Author Manuscript

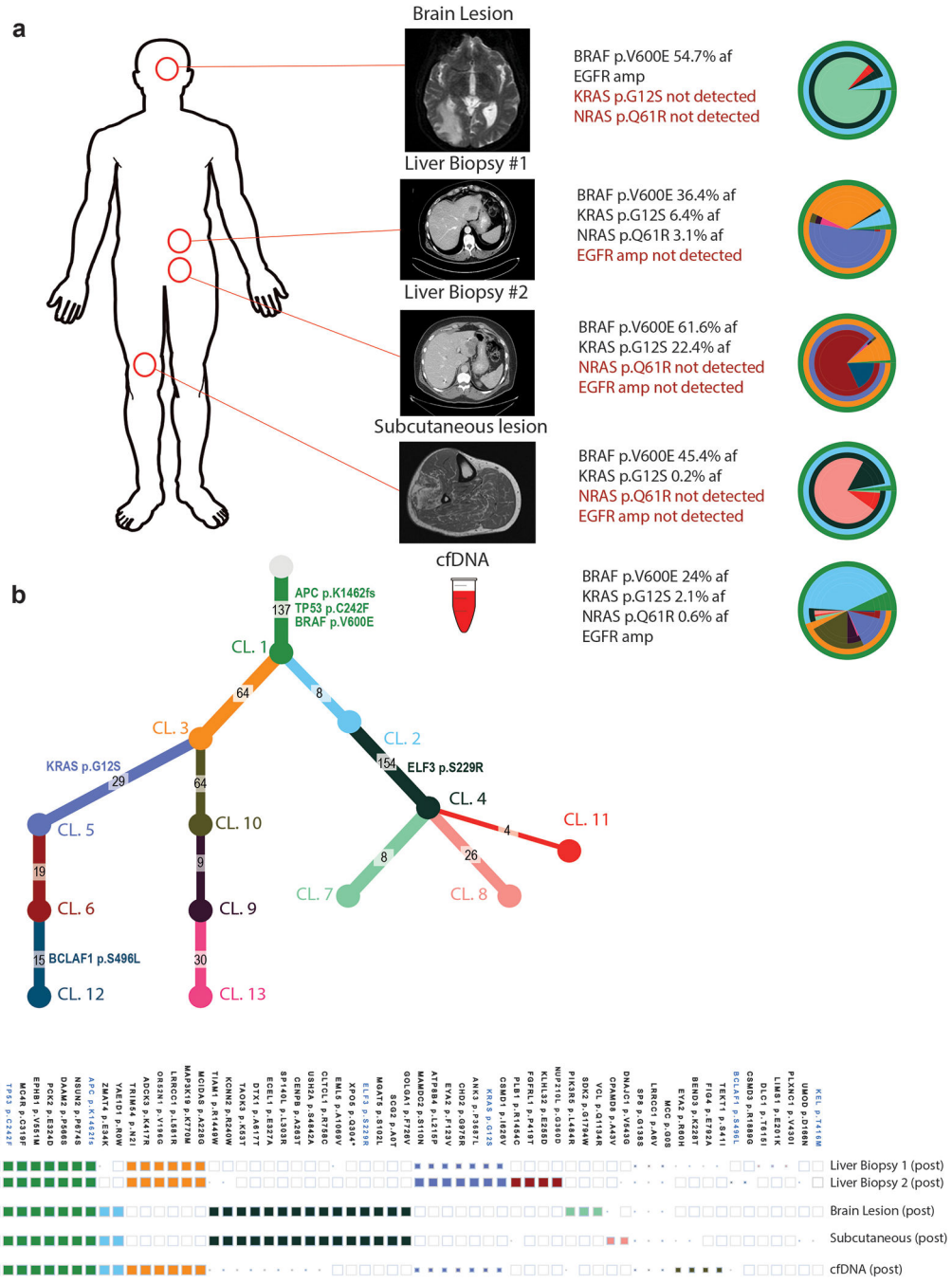

Figure 2: Comparison of multiple tumor biopsies versus liquid biopsy in a *BRAF*-mutant colorectal cancer patient.

(a) cfDNA (N=1) and tumor tissue biopsy specimens (N=4) included in the analysis for patient TPS037. For each specimen, the alterations and associated allelic fractions as determined by either ddPCR, targeted NGS, or WES are shown (Supplementary Tables 3–5). All ddPCR analyses were performed to a minimum coverage depth of 300X. Layered pie charts represent likely clonal composition of each specimen with the color of each subclone matching the color of the respective gene and branch in the phylogenetic tree. (b) Phylogenetic tree representing clonal architecture present in the specimens (using

Author Manuscript Author Manuscript Author Manuscript Author Manuscript

PhylogicNDT[44]). The number of somatic alterations assigned to each cluster and detected events in known cancer genes appear on the branches. (c) Representative clonal and subclonal coding somatic alterations detected in each plasma or tissue specimen. Size of each square represents the estimated cancer cell fraction of each alteration with an empty box indicating no detection. Events in known cancer genes are highlighted in blue.

Author Manuscript Author Manuscript Author Manuscript Author Manuscript

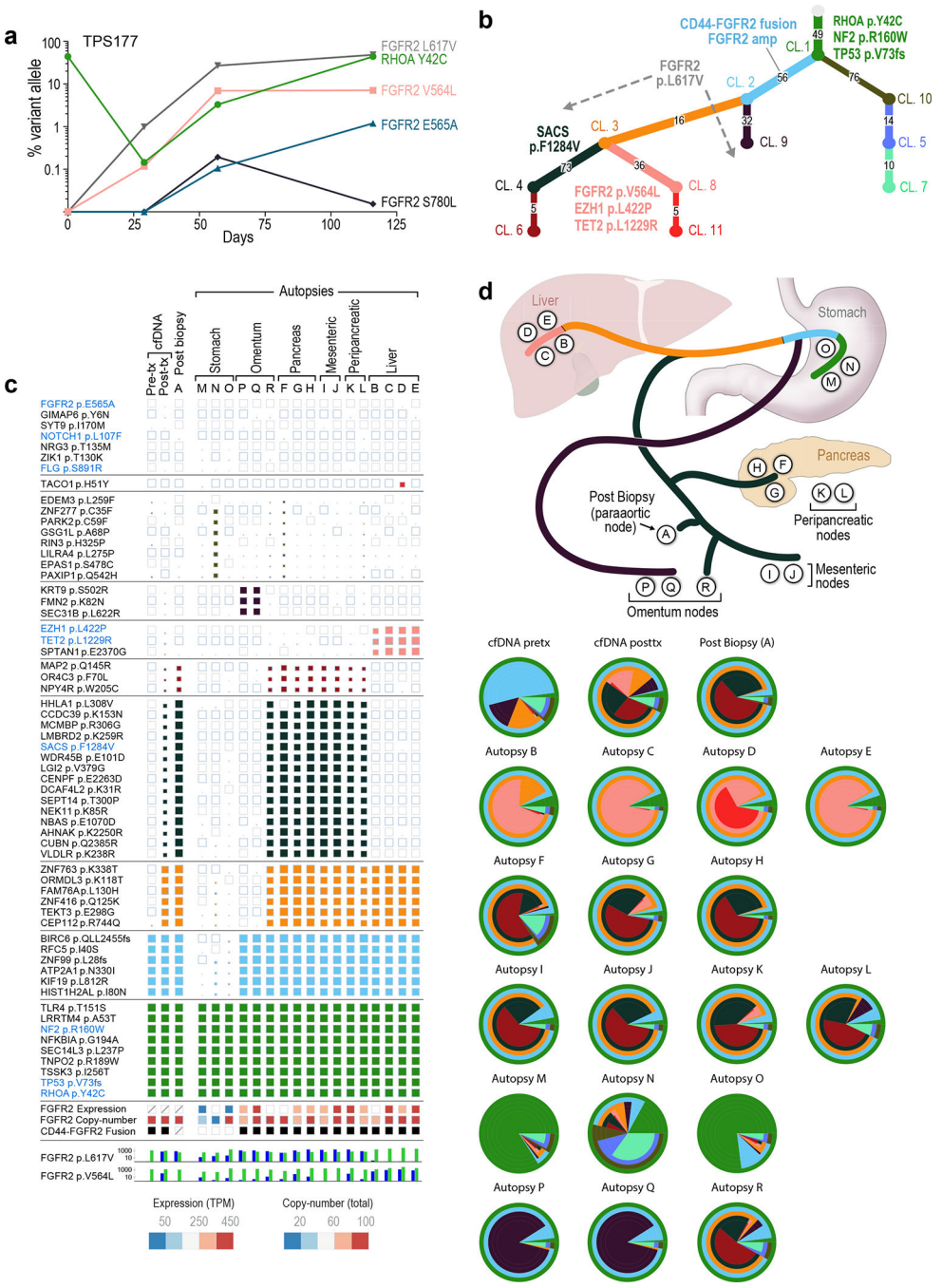

Figure 3: Serial liquid biopsy and autopsy in an *FGFR2*-fusion positive gastric cancer patient.

(a) The allele fraction of specific alterations in cfDNA isolated from serial plasma specimens during therapy with *FGFR* inhibitor were assessed by ddPCR to a minimum coverage depth of 300X. A truncal $RHOA^{Y42C}$ mutation is shown in green. Emergent candidate resistance alterations are also shown. (b) Phylogenetic tree representing clonal architecture across all specimens. The number of somatic alterations assigned to each cluster and detected events in known cancer genes appear on the branches. *FGFR2*-fusion and amplification events have likely occurred in the cyan subclone 2 (based on expression and copy-number patterns).

Author Manuscript Author Manuscript Author Manuscript Author Manuscript

FGFR2^{L617V} mutations are found at high levels in subclones 4 and 9. (c) Clonal and subclonal alterations detected in each plasma (N=2), tumor biopsy (N=1), or autopsy specimens (N=17). Size of each square represents the estimated cancer cell fraction of each alteration with an empty box indicating no detection. *FGFR2* expression (TPM), copy number (CN), and the presence of supporting *CD44-FGFR2* fusion reads as determined by WES and RNAseq are shown, along with the number of reads for the two major *FGFR2* resistance mutations (blue = mutant, green = wild type). Boxes with diagonal lines indicate no RNAseq data available. *FGFR2* fusions were confirmed in the cfDNA samples based on off-target WES reads. (d) Diagram of the locations of autopsy specimens included in the analysis with likely clonal migration patterns across lesions. Layered pie charts represent the estimated clonal composition of each specimen with the color of each subclone matching the respective gene color in the branch of phylogenetic tree.